1 July 2001

ELSEVIER

Optics Communications 194 (2001) 17–32

OPTICS COMMUNICATIONS

www.elsevier.com/locate/optcom

Method for measurement of the hemispherical/hemispherical reflectance of photovoltaic devices

Antonio Parretta [a,*], Haruna Yakubu [a,1], Francesca Ferrazza [b]

[a] *ENEA Centro Ricerche, Località Granatello, I-80055 Portici, Napoli, Italy*
[b] *Eurosolare SpA, Via D'Andrea 6, I-00048 Nettuno, Roma, Italy*

Received 21 November 2000; received in revised form 21 February 2001; accepted 28 March 2001

Abstract

A novel method and a relative apparatus, which allow the study of the reflectance properties at diffuse light of photovoltaic (PV) devices, are presented. The optical apparatus is provided with a 40 cm diameter integrating sphere (IS) which works like a lambertian source of diffuse light and, at the same time, collects diffuse light reflected by the sample. The reflectance measurements are based on the fact that the illumination intensity of the IS depends, besides on the input light power, also on the average reflectivity of its internal surface and then on the reflectance properties of any sample held against one of its apertures. The hemispherical/hemispherical reflectance, R_{hh}, of the sample under test is obtained by measurements of light irradiance inside the sphere in correspondence with the sample and with a selected number of standards of diffuse reflectance. The described method was used to optically characterise prototype PV modules (to be used in buildings), realised by encapsulating different types of normal and "gridless" monocrystalline-Si (mono-Si) and multicrystalline-Si (multi-Si) cells with different colours. The reflectance of the optically active area of the prototype modules was measured and the optical effect of the grid evaluated. Also the optical loss at diffuse white light was found to be approximately 4–5% for the mono-Si cells and 6–9% for the multi-Si cells. The quantity R_{hh}, when measured for very heterogeneous samples, such as multi-Si or poly-Si solar cells can be taken to represent the optical loss of the PV device operating outdoors, in the absence of sun tracking. This method, and the corresponding apparatus, can be extended to measurements on different plane surface samples.

PACS: 07.60.Hv; 42.85.Fe; 84.60.Jt

Keywords: PV modules; Optical losses; Integrating spheres

1. Introduction

The study, by theoretical and experimental means, of the optical properties (reflectance, transmittance, absorptance) of photovoltaic (PV) materials and devices, helps in predicting the optical losses of the PV devices when they are operating under outdoor irradiation conditions [1–12].

* Corresponding author. Tel.: +39-081-7723262; fax: +39-081-7723344.
E-mail address: parretta@portici.enea.it (A. Parretta).
[1] Present address: Department of Physics, University of Cape Coast, Cape Coast, Ghana.

0030-4018/01/$ - see front matter
PII: S0030-4018(01)01221-4

The optical loss represents one of the five "energetic losses" experienced by a PV module operating outdoors [13–23]. Two types of optical losses are distinguished in a PV device (generally a module) operating outdoors: a loss at direct light and a loss at diffuse light. The loss at direct light has been the subject of many investigations, mainly by simulation methods [24–29]. No results are available regarding the measurement of the optical loss under diffuse illumination. Also the study of light confinement in PV materials and devices [30–37] could be improved by reflectance and transmittance measurements under diffuse illumination. Purpose of the present work is to present an experimental method for the direct measurement of the reflectance of a plane surface sample under diffuse illumination. The reflectance is expressed by the quantity R_{hh} ("hh" is for "hemispherical/hemispherical") and is a measure of the total light reflected by the sample under an isotropic diffuse irradiation, extending to 2π steradians. The quantity R_{hh} could be derived, in principle, by measurements of directional/hemispherical (d/h) reflectance, $R_{dh}(\theta,\phi)$ [38,39], after integration over the incident angle θ and the azimuth angle ϕ (see Appendix A).

Most PV devices, like those fabricated from crystalline silicon with textured surface, show, however, anisotropic optical properties with respect to the azimuth ϕ (see Refs. [40, p. 128; 41, p. 235]). The calculation of R_{hh}, in this case, requires several measurements of the d/h quantities, taken at different incident and azimuth angles and a final numerical integration (see Appendix A).

Respect to this long hypothetical procedure, the method presented here for obtaining R_{hh} is very simple [42]. It requires an Integrating Sphere (IS) as source of diffuse light. At this purpose, the sphere must be adequately illuminated by an external collimated light source, with the sample under test facing an aperture of the IS. The illumination level inside the IS is then measured by means of an appropriate photodetector. By comparing the photodetector signal measured for the test sample with those measured for a set of standards of diffuse reflectance, the R_{hh} can be simply derived. The R_{hh} method is described in detail in Section 3.

If the spectrum "s" of the light source resembles that of the diffuse component of real solar radiation, then $R_{hh}(s)$ precisely gives the fraction of diffuse light lost by the module when placed horizontally on the ground (tilt $= 0°$). When the module is installed vertically respect to the ground (tilt $= 90°$), it is illuminated by both the diffuse light coming from the π sr portion of the sky and by the reflected light (albedo) coming from the π sr portion of the ground. The albedo component, for our purposes, can be considered equivalent to an isotropic source of light [43–45]. If "s_1" represents the spectrum of light from the sky and "s_2" that from the ground, then $R_{hh}(s_1)$ measures the loss of light from the sky portion and $R_{hh}(s_2)$ measures the loss of light from the ground portion. These are the only two experimental conditions for which the optical loss of the module can be precisely simulated by measurements of R_{hh}. For conditions different from tilt $= 0°$ and tilt $= 90°$, the optical loss can be evaluated by appropriate models [43,46,47].

The $R_{hh}(s)$ reflectance of a PV module at a standard spectrum of light can be taken as a parameter for comparing modules of different fabrication technologies, with a view to establish those most suitable for working with high intensities of diffuse light. These conditions are encountered at high latitudes, in countries where the sky is generally covered, or where the installation conditions of the modules are rather unfavourable in such a way as to make the diffuse light a relevant part of the total incident light [48].

As the application of our $R_{hh}(s)$ measurements is for the evaluation of the optical loss of PV modules when installed outdoors, we will refer to the standard solar light spectra to choose the appropriate light source for the measurements. At this purpose, only two diffuse light spectra have been considered, that is those corresponding to a clear-sky and to a covered-sky condition, with the simplified assumption of an isotropic radiance in both cases. The spectrum for diffuse light at clear-sky conditions can be derived by the standard AM1.5 direct normal and global spectra (ASTM, E892-87). No standard spectra for covered-sky conditions are available. There are, however, experimental evidences that lightly overcast sky

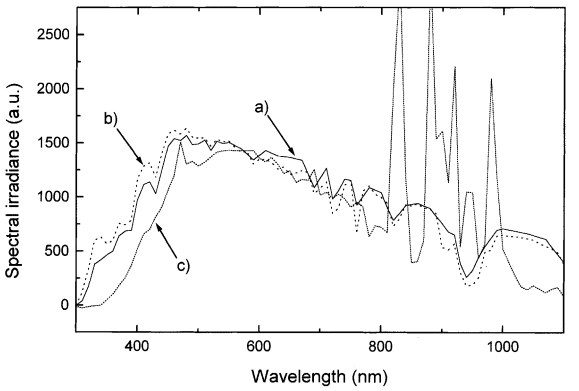

Fig. 1. (a) Standard AM1.5 global light spectrum. (b) Experimental spectrum of the global light measured under covered-sky conditions at the Portici site. (c) Spectrum of the Xe arc lamp used for the white-light h/h reflectance measurements. (Spectra b and c were enhanced for a better comparison with the spectrum a).

shows a spectrum of light close to the standard AM1.5 global one (see Fig. 1). The standard AM1.5 global spectrum, therefore, can be chosen as reference for simulating irradiation from lightly overcast sky [49].

Even if the distribution of the diffuse solar radiation over the sky hemisphere can undergo strong variations, anyway, the only viable approach to simulate it in laboratory is to produce an isotropic source of diffuse light, with a spectrum modulated in such a way to resemble one of the two standards spectra taken as reference.

In this paper we present the results of R_{hh} at monochromatic light, R_{hh} (633 nm), and at the white light of a Xe arc lamp whose spectrum is similar to the standard global irradiation AM1.5 (see Fig. 1). In this case we are able to simulate the optical loss of PV modules under covered-sky irradiation.

2. Experimental

2.1. Samples

A set of five Labsphere gray standards, 3 in. in diameter, were used as references for the R_{hh} measurements: SRS-40-030, SRS-20-030, SRS-10-030, SRS-05-030 and SRS-02-030, of nominal 8°/hemispherical reflectance: 40%, 20%, 10%, 5% and 2%, respectively. The diffuse gray standards are obtained blending different kinds of pigments with the white Spectralon material (a Teflon based polymer of $\geqslant 99\%$ 8°/h reflectance). The blending reduces the high lambertian character of the white Spectralon [50]. As a consequence, the d/h reflectance of the gray standards will not be perfectly constant with the incident angle θ [51,52].

For carrying out precise measurements on the optically active (o.a.) area of the cells, that is on the area not covered by the grid, and for evaluating the effect of the grid in modules with normal cells, special modules were fabricated by Eurosolare. The prototype modules were prepared by encapsulating together mono-Si and multi-Si cells, electrically unconnected. The multi-Si cells were of different colorations: blue, green, yellow-gold and violet. Two types of modules were fabricated: a first prototype, ES18GL, made up of cells without grid ("gridless" cells, or gl-cells); a second prototype, ES18G, made up of similar cells, but provided with grid. Both the mono-Si and the multi-Si cells were textured by the classical anisotropic chemical etching process (see Refs. [40, p. 128; 41, p. 235]).

2.2. Instrumentation

The h/h reflectance measurements were carried out by using an apparatus called HEmispherical–HEmispherical REflectometer (HERE) (see the schematics in Fig. 2). It is based on the use of a 40 cm in diameter IS, built by MACAM Photometrics. The port (w1) of the IS is used for the input of light from the source (l). The diametrically opposite port (w2) is used for holding the sample under test against it during measurements. Sources of light were He–Ne lasers ($\lambda = 633$ nm; $P = 1$–20 mW) and arc (Xe, Hg) lamps ($P = 150$–300 W). Xe arc lamps produce light with a spectrum similar to that of the solar radiation, as discussed, apart from some peaks typical of the Xe(I) and Xe(III) ions emissions (see Fig. 1). The spectrum of the Xe arc lamp light was measured inside the sphere by using the Oriel InstaSpec II PDA Spectrograph equipped with an Oriel Multispec monochromator (400 l/mm reticle). A Newport 4832-C multichannel

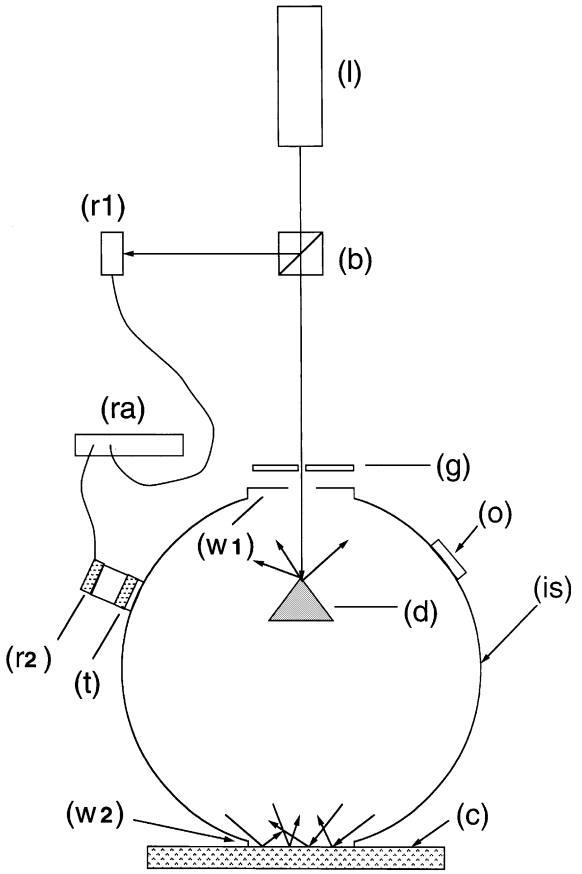

Fig. 2. Schematics of the experimental apparatus "HERE" used for hemispherical/hemispherical reflectance measurements on PV devices at laser light.

optical power meter, equipped with silicon photodiodes, was used for monochromatic ($\lambda = 633$ nm) light measurements. For measurements at white light, the silicon photodiode (r2) was replaced by a pyroelectric detector, as a flat spectral response is indispensable for these measurements (see Appendix A). The light detector system was a Laser Precision Rk-5720 Power Ratiometer, equipped with the RkP-575 pyroelectric detector. For measurements at white light, a lock-in configuration is strictly necessary, as the sensitivity of the pyroelectric detectors is by far lower than that of a silicon photodiode. The light beam was mechanically chopped at 30 Hz. A LICOR Mod. LI-1800 portable spectroradiometer was used for the outdoor spectroradiometric measurements.

3. Principles of R_{hh} measurements

We refer to the apparatus schematised in Fig. 2 and suitable for measuring R_{hh} of both small and large samples (c). The diffuse light produced in the IS irradiates the sample (c) which in turn reflects back into the sphere a portion of this light equivalent to R_{hh}, contributing to the irradiance inside the IS. This irradiance, measured by the photodetector (r2), is a function of the reflectivity of all the portions of the IS internal surface, and in particular, of the reflectivity of (c). This simple consideration allows us to evaluate R_{hh} just by comparing the irradiance measured for the sample (c) with those measured for some standards of reflectance, with known R_{hh} values. This measurement of R_{hh}, therefore, is not a direct optical measurement like the d/h reflectance [38,39], but an indirect measurement. The effect at the basis of the R_{hh} measurement is the cause of the appearance of the so-called "substitution error" [53]. It appears during measurements of d/h reflectance, R_{dh}, when the sample is replaced with a standard of reflectance. The "substitution error", to be avoided in d/h measurements, is here ennobled in a sense, as it becomes the source of information about the h/h reflectance.

In R_{hh} measurements, the primary beam does not strike the sample (c) directly, as in d/h measurements, but is directed towards a diffuser (d) (see Fig. 2). This way, the information relative to the "state" of light in the primary beam, like direction and polarisation, is practically lost. The diffusing material of the IS (commonly multiple coatings of MgO or $BaSO_4$) almost completely destroys the polarisation of light at the first reflection (see Ref. [50, p. 37]). This means that the light source (l) of Fig. 2 can be any type of light, polarised or not. This is very different from the R_{dh} measurements, where it is of fundamental importance to know the light polarisation and direction of incidence [38,39]. The standards used in R_{hh} measurements are those of diffuse reflectance, normally used for d/h reflectance measurements, $R_{dh}(\theta)$. They are generally supplied and calibrated only for a specific angle, typically 8°, as this is the standard angle of incidence used in commercial spectrophotometers. This makes it possible to

remove, when necessary, the specular component of the sample reflection by opening a special window. If the standards are supposed to be ideal diffusers, then it is easy to show (see Appendix B) that $R_{hh}(\lambda)$ (or $R_{hh}(s)$) corresponds to $R_{dh}(8°,\lambda)$ (or $R_{dh}(8°,s)$). Precise angle-resolved spectral measurements on standards of diffuse reflectance [51, 52], indeed, show that these standards slightly deviate from an ideal behaviour, that is the total d/h reflectance, $R_{dh}(\theta)$, is not perfectly constant with θ but tends to slightly increase at high angles. This fact can have a serious impact on d/h measurements, but is negligible in h/h measurements. In terms of power, in fact, light incident at angle θ produces irradiance proportional to $\cos\theta$ on the receiving surface. For the R_{hh} measurements, therefore, the assumption that the standards behave like ideal diffusers is by far a good approximation.

By alternatively fixing the five standards against window (w2) (see Fig. 2), and measuring the corresponding signal by the photodetector (r2), it is possible to draw a calibration curve of irradiance vs. R_{hh}, like that reported in Fig. 3. The criterion for the choice of the standards is to cover the range of reflectance, within which the unknown value is expected to fall, in order to draw a well defined irradiance/R_{hh} curve.

The R_{hh} values in Fig. 3 correspond to monochromatic light ($\lambda = 633$ nm). The curve of irradiance vs. R_{hh} shows an underlinear behaviour and can be well fitted by a second-degree polynomial. For small variations of R_{hh} the corresponding variations of the irradiance in the IS can be assumed linear:

$$\Delta E = c_1 \Delta R_{hh} \tag{1}$$

where c_1 is a factor related to the light integration capability of the IS and is here assumed independent on λ. If monochromatic light is used, the current from the photodetector (r2) can be expressed as:

$$\Delta \mathscr{I} = c_2 \Delta E = c_2 c_1 \Delta R_{hh} \tag{2}$$

where c_2 is the spectral response of the photodetector (r2) and E is the irradiance on (r2).

The situation substantially changes when white-light measurements are carried out. In this case, in fact, c_2 is a function of the spectral distribution of the light: $c_2 = c_2(s)$, and Eq. (2) becomes:

$$\Delta \mathscr{I}(s) = c_2(s)\Delta E = c_2(s) c_1 \Delta R_{hh}(s) \tag{2a}$$

The variations of the photodetector signal are not linearly related to variations of R_{hh}, but depend on the spectral response of the photodiode itself. For these measurements, therefore, it is necessary to use pyroelectric detectors, which assure a flat spectral response.

To determine the R^c_{hh} of the sample (c), it is necessary to measure the signal by (r2) and to derive the corresponding R_{hh} value from the calibration curve, by a simple interpolation procedure. In this case the value of R^c_{hh} has to be interpreted as the equivalent h/h reflectance of an ideal diffuser.

As a result of variations on R_{hh}, the corresponding variations on the irradiance increase at increasing the dimension of the (w2) window, *Sc*. To increase the sensitivity of R_{hh} measurements, therefore, it is convenient to operate with high *Sc* values, relative to the total internal surface area of the IS. This means that the IS has to be projected looking at the dimension of the samples testing area. For small solar cells (few square centimetres), it is convenient to operate with a small sphere (10–15 cm in diameter). In principle, a small sphere could be suitable also for testing small areas of large samples, like the encapsulated cells of a PV module. However, due to the light trapping

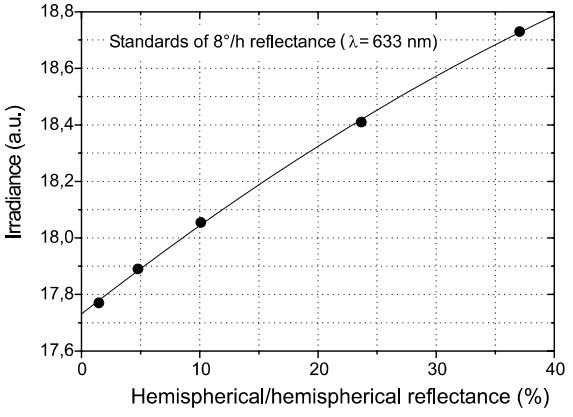

Fig. 3. Irradiance vs. h/h reflectance calibration curve obtained by measuring the irradiance produced on the photodetector (r2) of Fig. 2 in correspondence of five Labsphere standards of nominal 8°/h reflectance: 2%, 5%, 10%, 20% and 40%, respectively.

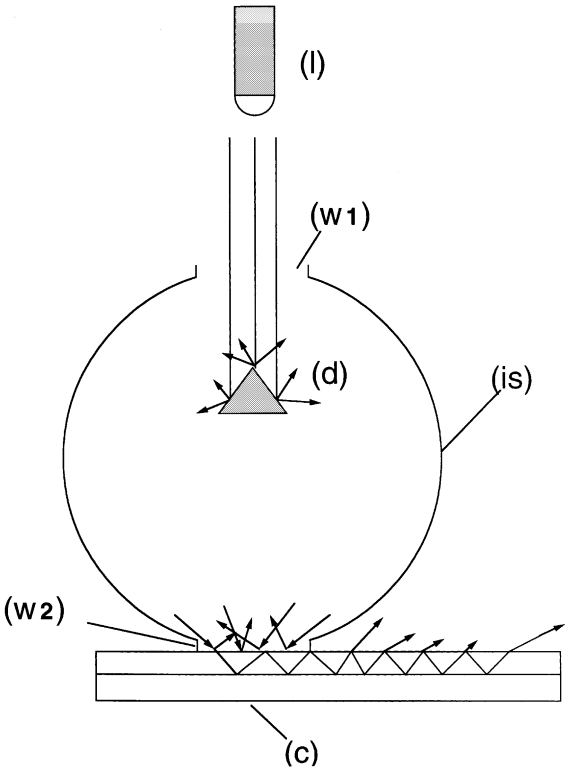

Fig. 4. Schematics of the reflectance apparatus evidencing the phenomenon of light trapping inside the cover glass of a PV module. A portion of the light incident on the sample exits from window (w2) and is not collected by the sphere. This portion of light changes at changing the dimensions of the collecting window (w2).

phenomenon occurring inside the glass cover, which extends for lengths well above the linear dimension of the window (w2) (see Fig. 4), a considerable amount of incident light is trapped inside the glass encapsulant, and exits from the sample out of the window (w2). As a consequence, measurements performed with too small collecting windows (w2), with respect to the real sample, are expected to underestimate the true reflectance experienced by the entire module. When testing single encapsulated cells of 10–12 cm in diameter or cells within PV modules, it is convenient, therefore, to work with an IS of 40–50 cm diameter.

There is another aspect of R_{hh} measurements which cannot be disregarded: the presence of the grid in the cells. The grid reflects the incident light, like the semiconductor region does, but only partially contributes to the light collection. In encapsulated cells, indeed, only a small portion of light, reflected by the grid, is back reflected by the glass/air interface towards the active material of the cell. In general, the grid affects the measurements resulting to an overestimation of reflectance of the o.a. region of the cell and then an overestimation of the optical loss [38,39]. In d/h measurements this problem can be overcome by using well collimated beams, possibly from laser sources, which impinge only on the region between two adjacent fingers [38,39]. In the present case, however, the incident light has a diffuse nature and the illuminated region must be relatively large, as discussed before, so the grid illumination cannot be avoided. To obviate this problem, special modules made of gridless cells were fabricated. The comparison between "normal" modules and modules with gridless cells can put in evidence the contribution given by the grid on the R_{hh} measurements. This will be discussed in details later in Section 5.

4. Project of the apparatus for R_{hh} measurements

4.1. Sources of diffuse light

The diffuse solar light, supposed isotropic, behaves like a lambertian light source [50]. With regards to the incident angle (θ) and the azimuth angle (ϕ), the radiance of this source, L ($W\,m^{-2}\,sr^{-1}$), is constant with respect to the different orientations in the sky. The radiance is defined as the irradiance produced on a unitary surface oriented perpendicularly in a particular direction and collecting light from a unitary solid angle (1 sr). If the receiving surface is kept horizontal, it will receive light, within a unitary solid angle, of maximum irradiance from the zenith and zero from the horizon. Consequently, this irradiance will change as the $\cos\theta$ function.

An IS can be used to simulate a source of diffuse light in the laboratory. Before demonstrating this, let us first consider the general case of an illuminated wall (s) surrounding the sample (c), centred at (O), in the entire hemisphere in front of it (see Fig. 5), and consider the irradiance E produced in (O). For simplicity, Fig. 5 shows only the section

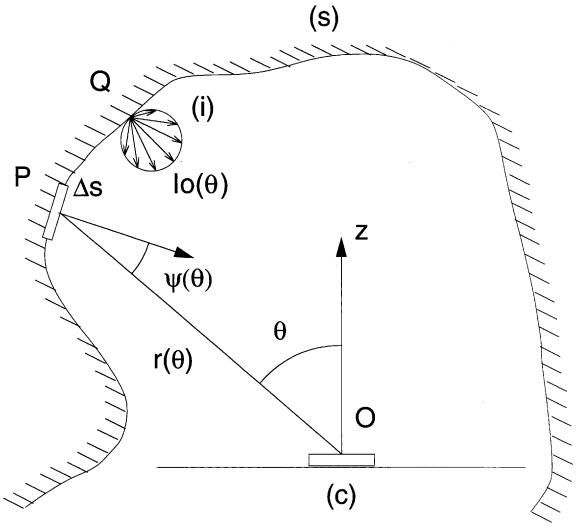

Fig. 5. General case of an illuminated wall (s) surrounding the sample (c). If the wall is homogeneously illuminated ($I_0(\theta) = \text{const}$), then the radiance on the sample is constant too and the wall is an ideal source of diffuse light.

of the irradiating surface that is orthogonal to the sample surface. Changing the azimuth angle ϕ, the orthogonal plane rotates around the z-axis and the same considerations can be applied to other ϕ angles. The irradiance produced in (O) by the surface element Δs, irradiating from the point (P), can be expressed as (see Ref. [50, p. 25]):

$$\Delta E(\vartheta, \varphi) = \text{const} I_0 \frac{\Delta s \cos\psi \cos\vartheta}{r^2} \ (\mathrm{W\,m^{-2}}) \qquad (3)$$

where I_0 is the intensity of light emitted (or reflected) by a unitary surface of the illuminated wall (s), r is the modulus of the vector joining the points (O) and (P), ψ is the angle the vector r forms with the normal to the Δs surface and θ is the angle the vector r forms with the normal to the receiving surface. I_0, ψ and r are functions of the angles θ and ϕ, which define a point on the irradiating surface. Additionally, with:

$$\Delta\Omega = \frac{\Delta s \cos\psi}{r^2} \ (\mathrm{sr}) \qquad (4)$$

being the solid angle within which the point (O) see the elementary Δs source, we can write:

$$\Delta E(\vartheta, \varphi) = \text{const} I_0(\vartheta, \varphi) \Delta\Omega(\vartheta, \varphi) \cos\vartheta \ (\mathrm{W\,m^{-2}}) \qquad (3a)$$

The "radiance" in (O) corresponds to the irradiance measured when the receiver is collimated to the source of light ($\cos\theta = 1$) and the solid angle is unitary ($\Delta\Omega = 1$):

$$L(\theta, \varphi) = \text{const} I_0(\theta, \varphi) \ (\mathrm{W\,m^{-2}\,sr}) \qquad (5)$$

If the light emitted by the wall is homogeneous, we have $I_0(\theta, \phi) = \text{const}$ and thus:

$$L(\vartheta, \varphi) = \text{const} \ (\mathrm{W\,m^{-2}\,sr}) \qquad (5a)$$

It comes out that, if light distribution in the sphere is homogeneous ($I_0 = \text{const}$) and the receiver faces the internal wall of the IS, whatever be its position and orientation inside the IS, the radiance on the receiver will always be constant with respect to the different directions from the front hemisphere (θ and ϕ angles). From Eq. (5a) it can be deduced also that the shape of the irradiating surface is irrelevant, when it radiates in a homogeneous way, for producing a constant radiance on (c). In the practice, as the wall (s) of Fig. 5 radiates by reflected light, in order to illuminate it as much as possible homogeneously, it is necessary to start from a spherical surface (IS).

Let us now discuss where to place the sample and how the sphere should be illuminated. Considering that the tested samples can be as large as a PV module, and that they are generally different from the standards of reflectance in dimension, it is excluded that the measurements could be carried out with the sample inside the sphere. Once defined the area of testing, it is necessary to provide the IS with a window of the same dimension, to which face the sample (c) and the standards (see Fig. 6a). When the light beam is directed into the IS, excluding the very luminous area where the light beam strikes the surface, the rest of the sphere is almost equally illuminated as an effect of light integration. The area where the input beam strikes the IS surface can be hidden from the testing area by using an appropriate baffle (see Fig. 6a). The presence of the baffle, however, determines a slight asymmetry in the light distribution over the sample. To obviate this, we decided to send the light beam against a diffuser (d) placed at the centre of

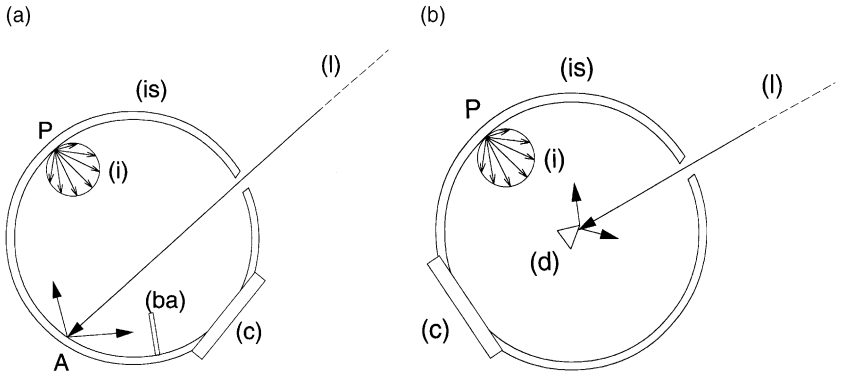

Fig. 6. (a) The figure shows an IS illuminated by a light beam striking its internal surface. Apart from the very luminous region near the point A, all the points P of the sphere wall irradiate light in a quasi-lambertian way. The indicatrix (i) of the diffusing element of the surface is indicated in P. A baffle is commonly used inside the IS to hidden the intense light spot from the testing area, assuring in this way a more homogeneous diffuse illumination of the sample. (b) A diffuser (d) is placed at the centre of the sphere. In this case it acts also as the baffle (ba) of Fig. 6a.

the sphere (see Fig. 6b). If the coating of the IS behaves like an ideal diffuser (Lambert-type radiator), the angular distribution of light intensity, emitted by any elementary portion of the surface, can be represented by a spherical surface (indicatrix) in contact with the radiating point (see Fig. 6a and b and Ref. [50, p. 29]).

We have experimentally verified that the configuration of Fig. 6b assures a constant radiance on the sample (c). Fig. 7 shows an IS illuminated by the source (l) through the window (w1). The light is directed towards the diffuser (d), which then diffuses the light and, in turn, reflects it into the sphere. A window (w2) is opened on the IS at a position diametrically opposite the source. A photodiode (p), inserted at the bottom of a telescopic tube (t), is used to measure the irradiance inside the sphere. The tube (t) enables the photodiode to receive light from only the internal surface of the sphere. It can be rotated around a vertical axis passing through the centre of (w2) and oriented at a variable angle (θ) with respect to the optical axis. The photodiode (p) always measured a constant signal at changing θ values, confirming the fact that the radiance produced by the IS source is constant when the receiver is placed at any aperture of the sphere. A further confirmation was obtained by removing (t) and measuring the signal directly by (p). In this case (p) sees the entire window (w2) and the signal precisely follows a $\cos\theta$ function (see Fig. 8).

4.2. The apparatus HERE

The apparatus for R_{hh} measurements is schematised in Fig. 2 for the case of a laser light source. By using a white-light source (Xe arc lamp), the scheme only changes for the fact that the light of the lamp has to be focused onto the diffuser (d). Care must be taken in this case to prevent the beam from striking the window (w1), and also to focus the light precisely onto the diffuser (d), otherwise shadowing effects will manifest in both cases, with a consequent lack of homogeneity of light distribution into the IS. The apparatus used for R_{hh} measurements at white light is shown also in the photographs of Fig. 9a and b. When single cells are to be characterised, they are fixed at the window (w2) which has a maximum diameter of 15 cm. For measurements on modules, these are fixed on a trolley (see Fig. 9b) which is moved towards the sphere, in such a way as to position the area under test precisely at the window (w2). The light from the source (l) is split up into two beams by the beam splitter (b) (see Fig. 2). One beam is measured by (r1) + (ra), where (ra) is a multichannel radiometer, and is taken as reference to control changes in the intensity of the

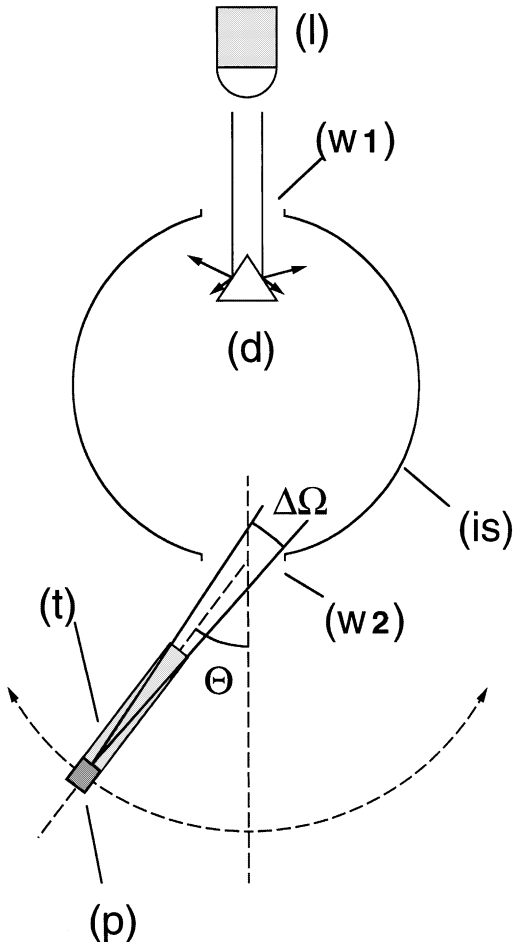

Fig. 7. Experimental set-up used for the measurement of the radiance of an IS. The detector (p) is looking only at the interior of the sphere.

light source. The second beam pass through the diaphragm (g) and enters the sphere through the window (w1) thereby striking the diffuser (d), placed near the centre of the sphere. The diffuser (d) is a $BaSO_4$ coated disk, the same as the internal surface of the IS. The irradiance inside the IS is measured by the photodetector (r2), placed into a small cylinder covered by a semi-transparent diffuser (t). The radiometer (ra) then collects the signals from the two detectors, (r1) and (r2), and works out their ratio. In this way the irradiance inside the IS is normalised with respect to the primary beam intensity. The detector (r1) can be a silicon photodiode for any type of measurements.

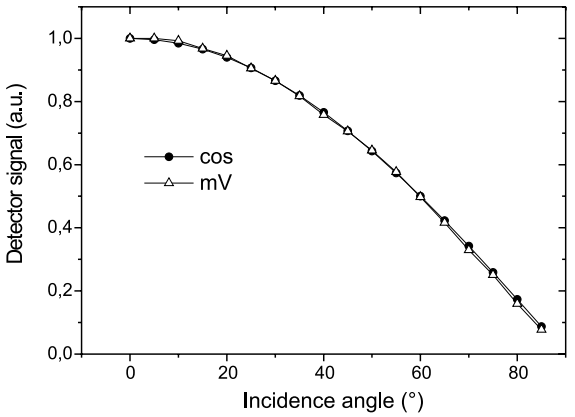

Fig. 8. The signal (see "mV" curve), measured by the detector (p) in the configuration of Fig. 7 when the tube (t) is removed, precisely follows the $\cos\theta$ function (see "cos" curve).

For monochromatic light measurements, (r2) can be a silicon photodiode too, but for white-light measurements it must be a pyroelectric detector. The view port (o) is used to adjust the position of the testing area towards the window (w2). The window (w2) is circular but can be masked to suit the particular shape of the sample. For measurements on encapsulated cells with grid, for example, it could be necessary to avoid the illumination of the wide and highly reflective bus bars. In this case, the mask is shaped in almost a rectangular form in order to expose to light only the region which lies between the two bus bars (Fig. 10).

For white-light measurements, a Xe arc lamp was used. The spectrum can be even modulated to better suit the distribution of the real diffuse irradiation, by using an appropriate set of filters. For spectral measurements, a band-pass filter (f) or a monochromator is placed between the source and the beam splitter (b).

5. Results of R_{hh} measurements

R_{hh} measurements have been carried out on prototype modules supplied by Eurosolare. The ES18GL prototype, made up of cells without grid, was first characterised using laser light. Fig. 11 shows the R_{hh} results for the different cells: mono-Si cells with blue colour and multi-Si cells with

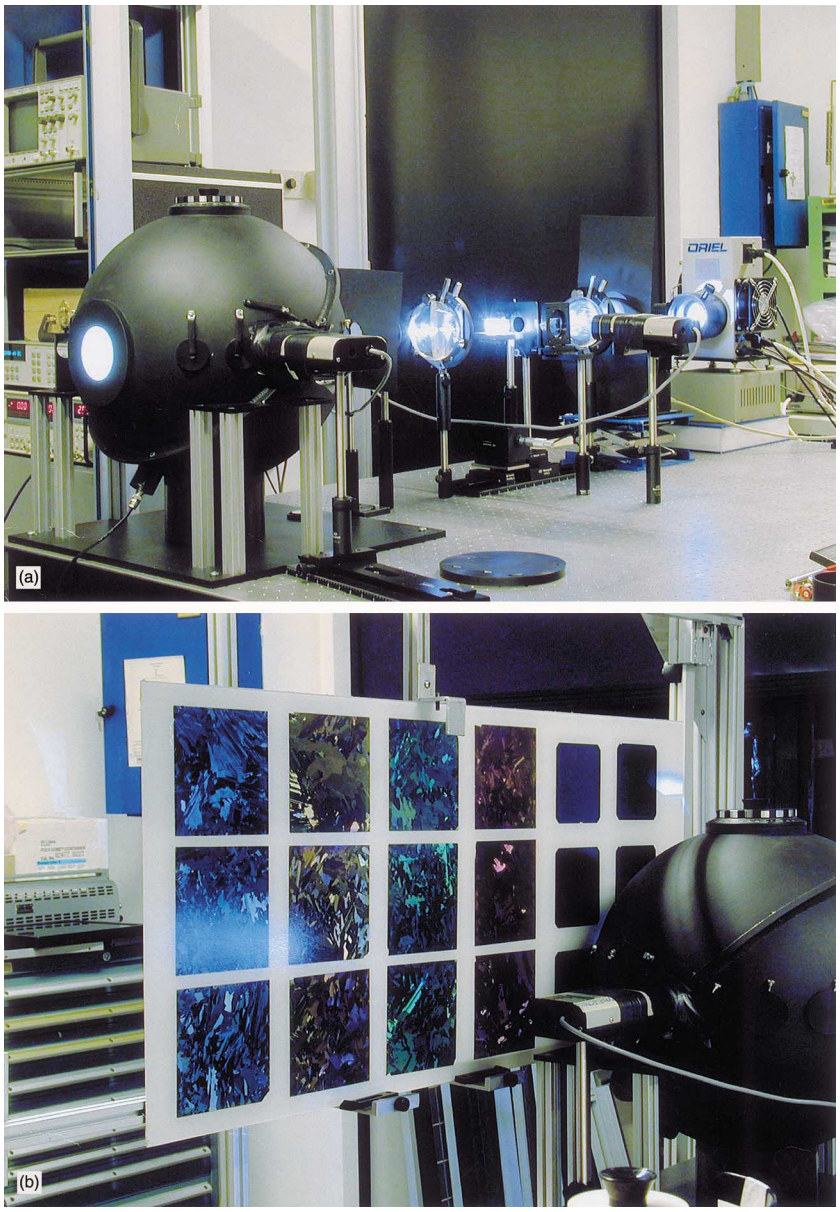

Fig. 9. The apparatus for R_{hh} measurements is shown in these photos. (a) General view of the apparatus. (b) Particular of the IS with a gridless cells module under characterisation.

different colours (blue, green, yellow-gold and violet). The data represent the average optical behaviour of the single cells. The mono-Si cells show the lowest R_{hh} value of 4–5% under red light. The multi-Si cells behave quite differently depending on the colour. The blue and green multi-Si cells show similar reflectance values, between the 5% and 7% interval. The yellow-gold and violet multi-Si cells show higher reflectance with values as high as 8–11%. Cells with the same colour show a significant dispersion of R_{hh} values due to the different crystallographic orientations of the crystals at the

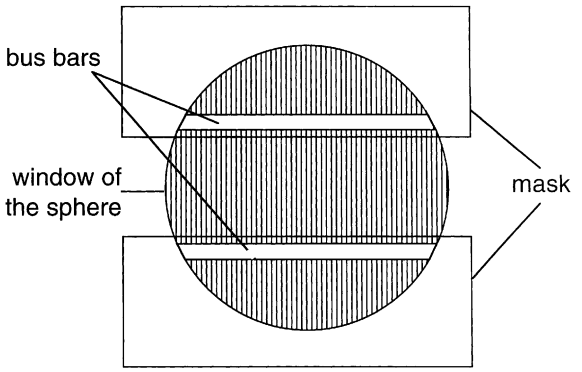

Fig. 10. It is shown a typical mask to be placed on a solar cell, when it is necessary to avoid the reflection from the bus bars.

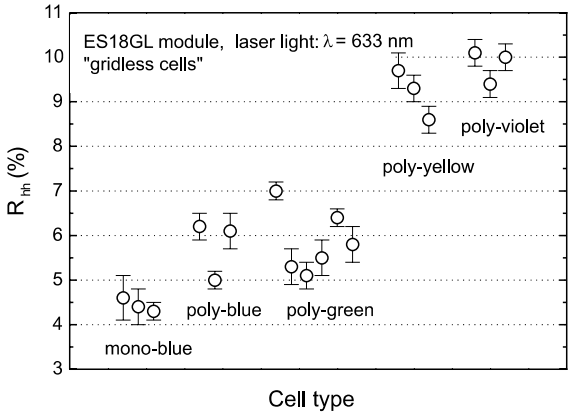

Fig. 11. Hemispherical/hemispherical (h/h) reflectance of the Eurosolare PV modules made of mono-Si and multi-Si gridless cells. The results refer to monochromatic light ($\lambda = 633$ nm). The multi-Si cells were processed in a different way to show different colouring at white light: blue, green, yellow-gold and violet.

surface of the cell, which manifests themselves differently with varying reflection properties. This means that the reflectance of a multicrystalline cell is strongly influenced by the crystalline substrate, even if the antireflection coating (ARC) process was the same for cells with the same colour. The different crystalline substrates, with their different crystallographic orientation, could also have induced a different growth velocity of the ARC, during the deposition process.

The strong heterogeneity of the multi-Si cells makes the evaluation of the grid effect on the R_{hh}

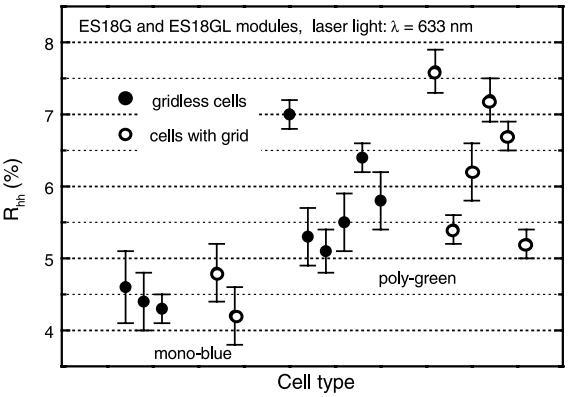

Fig. 12. Comparison between the (h/h) reflectance of normal and gridless cells modules. Only the results for the blue mono-Si and green multi-Si modules are here reported.

reflectance rather difficult. This is shown in Fig. 12, where the reflectance results of gridless mono-Si cells and green multi-Si cells are compared to those of the corresponding cells provided with grid. For the blue mono-Si cells the effect of the grid is small and hidden by the dispersion of the R_{hh} values measured for the gridless cells. For the green cells with grid, there is a dispersion of R_{hh} values slightly higher than for the corresponding gridless cells, and an increase of the average value of 0.5–1%. The maximum effect of the grid on the R_{hh} measurements for multi-Si cells seems, therefore, to be of the order of 1%, which is well below the dispersion of the R_{hh} values themselves (≈3%). We conclude that Eurosolare PV modules could be characterised taking roughly into account a 1% increase in the reflectance, as grid effect, for that particular grid design.

Using diffuse white light the gridless cells reflect as shown in Fig. 13. With respect to monochromatic light measurements, very different results are observed, as expected. The blue mono-Si cells again show the lowest optical losses (4–6%), whereas the multi-Si cells show now reflectances in the 6–9% interval, much less colour dependent than under red light. The highest reflectance is attained with the violet and yellow-gold coloured cells, the same that produced the highest optical loss at red light.

Considering the results obtained under both monochromatic (red) and white light, we expect

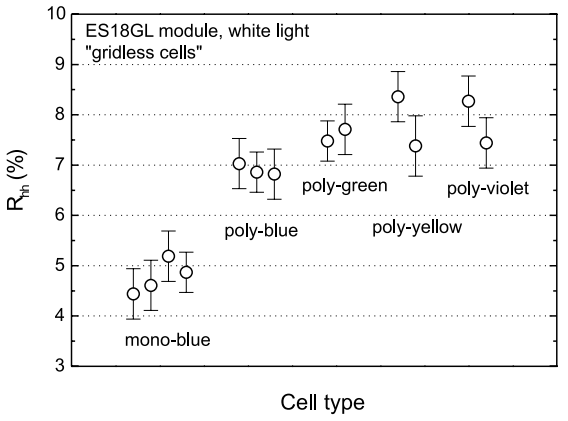

Fig. 13. Hemispherical/hemispherical (h/h) reflectance of the gridless cells of the ES18GL Eurosolare PV module, at the white light produced by a Xe arc lamp.

that, among the different multi-Si cells, the blue and green-coloured cells should be preferred, as far as the electrical performance of modules is taken into account. Their lower optical loss under red light, in fact, determines a higher current production at white light, as the spectral response of a silicon cell increases with increasing wavelength (see Ref. [40, p. 165]). These results must be taken into account when making a choice from the differently coloured Eurosolare m-Si modules.

An interesting fact to be noted is that the dispersion of R_{hh} values, for a given type of multi-Si cell, is a little higher for monochromatic (red) light than for white light (1.5–2% against 1–1.5% respectively). It seems that the optical heterogeneity of the multi-Si cells is attenuated by white light, or, equivalently, that the monochromatic light loss of the multi-Si cells is more sensitive to the different crystallographic orientations of the silicon surface crystals.

6. Discussion about the method

The reflectance method discussed here gives the average reflectance of large tested areas of a solar cell. It is thus very suitable for characterising multi-Si cells, which manifest very different local optical properties within the single cell and from cell to cell. Only a method intrinsically meant for "large areas" could be applied to the optical characterisation of multi-Si cells, for which a "punctual" characterisation does not make too much sense. We can even push far this concept affirming that, perhaps, the most practical and simplest way to summarise the optical reflectance properties, or optical loss, of multi-Si cells or multi-Si materials in general, could be just to assign their h/h reflectance, R_{hh}. This approach appears convincing dealing with diffuse light irradiation. Thinking of alternative, practical methods for measuring the optical loss of a multi-Si material using collimated light, in alternative to diffuse light, traditional methods of reflectance measurement imply the testing sample being illuminated by a small cross-section beam, always internal to the sample surface. The overall optical reflectance behaviour of the sample is therefore missed by these measurements. Moreover, larger regions of the sample, with different optical properties, are illuminated when the incidence angle of the beam is increased, with a consequent loss of congruence in the set of measurements. The recently published method called differencing reflection method (DRM) [51,52,54], developed by us, could be an alternative to the present R_{hh} method when investigating multi-Si materials by collimated beams, without loosing the overall information contained in the optically heterogeneous cell material. This method, in fact, entails the use of a large, collimated light beam, illuminating the entire surface of the sample at any chosen angle of incidence. Also, this innovative method proves to be suitable for characterising strongly heterogeneous materials or devices, giving the average reflectance of the sample at a particular angle of incidence. The DRM method seems suitable for assigning the optical loss of a heterogeneous PV device, which operates constantly at a specific angle with respect to the light source, for example 0° when the device is tracking the sun disk. The characterisation of large multi-Si cells (10–12 cm in size) by DRM, however, would imply the use of large IS, about 60 cm in diameter, to maintain a proportionality factor between sample and the size of sphere [51,52,54]. Considering that an installed PV device is generally oriented towards a fixed direction outdoors, it experiences a

wide range of incidence angles of light, and the only d/h reflectance at 0°, $R_{dh}(0°)$, is not so representative of the average outdoor optical loss of that device, in this case. More representative could be $R_{hh}(s)$, as it better summarises outdoor reflectance properties, and also takes into account the fact that the diffuse component of the outdoor solar radiation can be relevant in some cases [20].

The fact that the h/h reflectance, $R_{hh}(s)$, of a multi-Si PV device could be taken as a representative parameter of its optical loss, when outdoor and no-tracking operation is considered, seems now convincing.

For sun-tracking operation, the most suitable parameter of its optical loss could be the d/h reflectance, $R_{dh}(s, 8°)$, or more simply $R_{dh}(s, 10°)$, easily derived by our ROSE or DRM apparatuses. We have excluded the 0° reflectance, $R_{dh}(s, 0°)$, which is more difficult to be measured by our apparatus as the specular beam exits out of the input port for this incident angle.

7. Validation test

To make an estimation of validity of our R_{hh} measurements, the R_{hh} reflectance was also calculated by using the d/h reflectance data, R_{dh}, as established by Eq. (A.1a) Fig. 14 shows the $R_{dh}(633, \theta)$ data obtained for a blue-coloured mono-Si cell of the ES18GL module, at monochromatic light ($\lambda = 633$ nm). The data were fitted by a fifth and sixth degree polynomial after having put $R_{dh}(633, 0°) = R_{dh}(633, 10°)$ and $R_{dh}(633, 90°) = 100\%$. A calculated value of $R_{hh}(633) \approx 4\%$ was obtained in both cases, to be compared with the experimental value of $R_{hh}(633) = 4.6 \pm 0.5\%$. The agreement between experimental and calculated data can be accepted as good. Some little experimental effects have been picked out, which have likely produced the above little underestimation of the calculated h/h reflectance:

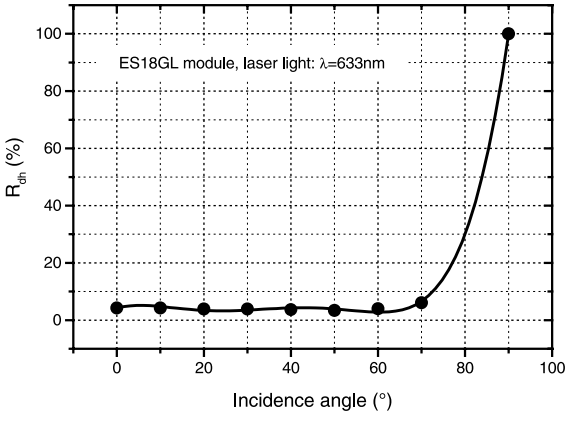

Fig. 14. Curve of directional/hemispherical (d/h) reflectance, $R_{dh}(633, \theta)$, at red light ($\lambda = 633$ nm), measured by our ROSE apparatus for the blue mono-Si module.

(i) The $R_{dh}(633, \theta)$ curve has been obtained for only one azimuth angle of the incident light [39], that one defined by the plane orthogonal to the mono-Si cell surface and parallel to one side of the square base of the random pyramids produced by the anisotropic chemical etching (see Section 2). Previous reflectance measurements on pyramidal texturisations [39] have shown that the reflectance shows a minimum at this azimuth angle.

(ii) The $R_{dh}(633, \theta)$ measurements have been carried out with a window of small diameter (3 cm) in order to limit the substitution error, the basis of the present method (see Section 3). The experimental $R_{hh}(633)$ measurements, on the contrary, have been carried out with a 7.5 cm diameter window. As a consequence, the $R_{dh}(633)$ measurements could have dispersed more light out of the window, with respect to the $R_{hh}(633)$ measurements, as an effect of light trapping in the module cover glass (see Fig. 4). The final effect of this light trapping in the encapsulant, could be an underestimation of $R_{dh}(633, \theta)$, and finally of the $R_{hh}(633)$ calculated by it.

(iii) Data of $R_{dh}(633, \theta)$ from 70° to 90° are not available.

From what was discussed before, it appears clear that, in order to validate our method, it is not possible to over emphasise the comparison between the h/h results obtained experimentally and those calculated by the experimental d/h measurements. This is because the experimental d/h measurements, required in principle to get precisely calculated h/h reflectance, could be so many to require too much work. Secondly, the propagation of the corresponding errors could lower the

precision required for the "validation" method. It remains important to focus on the fact that the experimental h/h measurements by the HERE apparatus do give results, which agree with those calculated by representative d/h measurements. The present method, moreover, implies a measurement procedure so simple that systematic errors could only be derived by a loss of accuracy of the reflectance standards. These, however, are supplied with certified values and have shown a good similarity with ideal light diffusers.

8. Conclusions

In conclusion, a method and the relative apparatus (both shortly called as HERE) have been presented, which make it possible to measure the hemispherical/hemispherical reflectance, R_{hh}, of any plane surface and, in particular, of PV materials and devices (solar cells, modules). The method is based on a procedure that is simple and non-destructive. The basis of the apparatus requires the use of an IS, typically of 30–40 cm diameter. The R_{hh} measurements directly give the optical loss of a PV device under diffuse illumination. This loss, together with that measured for the direct light, expresses the total optical loss of a PV device, one of the five effects which contribute to define its outdoor performances. The basic apparatus here presented is suitable for characterising both small and large samples.

The HERE method can work on testing areas as high as tenths of square centimetres. It is thus particularly suitable for characterising multi-Si devices, which are intrinsically highly heterogeneous from point to point. The method gives the average optical reflectance at diffuse light of a multi-Si cell, when the use of a directional/hemispherical method would require lots of measurements at different incident angles.

We can affirm that the R_{hh} datum can be taken as representative of the optical loss of a PV devices operating in outdoor conditions, in absence of sun tracking. For sun tracked PV devices, other methods of optical loss characterisation, like the DRM (see text), could be used to better represent the optical loss of the modules.

The measurement of special modules made of gridless cells, allowed us to determine the optical loss manifested at diffuse light by the o.a. region of the cells. Losses of 4–5% for modules made of mono-Si cells and of 6–9% for modules made of differently coloured multi-Si cells were measured by our method at white light.

Acknowledgements

The authors acknowledge G. Leanza and S. Ferlito for the measurements of light spectra. The work was done with the financial support of the Italian Ministry of University and Technological Research (MURST).

Appendix A

The hemispherical/hemispherical (h/h) reflectance, R_{hh}, can be calculated by the directional/hemispherical (d/h) reflectance, $R_{dh}(\theta,\phi)$, integrating over the incident angle θ and the azimuth angle ϕ:

$$R_{hh}(\lambda) = \frac{\int_0^{2\pi} d\varphi \int_0^{\pi/2} d\vartheta \sin\vartheta\cos\vartheta R_{dh}(\lambda,\vartheta,\varphi)}{\int_0^{2\pi} d\varphi \int_0^{\pi/2} d\vartheta \sin\vartheta\cos\vartheta} = \cdots \frac{1}{\pi}\int_0^{2\pi} d\varphi \int_0^{\pi/2} d\vartheta \sin\vartheta\cos\vartheta R_{dh}(\lambda,\vartheta,\varphi) \quad (A.1)$$

where λ is the wavelength of the incident light. Eq. (A.1) represents the spectral h/h reflectance.

If the incident light is not monochromatic, but spread over a range of wavelengths with spectral irradiance $E(\lambda)$ (spectrum "s"), an equivalent equation can be written:

$$R_{hh}(s) = \frac{1}{\pi}\int_0^{2\pi} d\varphi \int_0^{\pi/2} d\vartheta \sin\vartheta\cos\vartheta R_{dh}(s,\vartheta,\varphi) \quad (A.2)$$

where

$$R_{dh}(s,\vartheta,\varphi) = \frac{\int_s d\lambda E(\lambda) R_{dh}(\lambda,\vartheta,\varphi)}{\int_s d\lambda E(\lambda)} \quad (A.3)$$

If, however, the sample is isotropic with respect to ϕ (or can be approximated as an isotropic

sample), that is if R_{dh} is a function of only θ, then Eqs. (A.1) and (A.2) can be simplified as:

$$R_{hh}(\lambda) = 2\int_0^{\pi/2} d\vartheta \sin\vartheta\cos\vartheta R_{dh}(\lambda,\vartheta) \quad (A.1a)$$

$$R_{hh}(s) = 2\int_0^{\pi/2} d\vartheta \sin\vartheta\cos\vartheta R_{dh}(s,\vartheta) \quad (A.2a)$$

where

$$R_{dh}(s,\vartheta) = \frac{\int_s d\lambda E(\lambda)R_{dh}(\lambda,\vartheta)}{\int_s d\lambda E(\lambda)} \quad (A.3a)$$

$$R_{hh}(s) = \frac{\int_s d\lambda E(\lambda)R_{hh}(\lambda)}{\int_s d\lambda E(\lambda)} \quad (A.4)$$

The integrals in Eqs. (A.1)–(A.3) or Eqs. (A.1a)–(A.3a) can be evaluated by numerical methods applied to the d/h reflectance data.

Appendix B

We demonstrate that the hemispherical/hemispherical (h/h) reflectance, $R_{hh}(\lambda)$ or $R_{hh}(s)$, of an ideal diffuser corresponds to the directional/hemispherical (d/h) reflectance, $R_{dh}(8°,\lambda)$ or $R_{dh}(8°,s)$, of the same diffuser, where λ is the wavelength of a monochromatic light and s is the spectrum (spectral irradiance) of a white light. We re-write Eq. (A.1a), which can be applied to samples whose optical properties are isotropic with respect to the azimuth angle ϕ:

$$R_{hh}(\lambda) = 2\int_0^{\pi/2} d\vartheta \sin\vartheta\cos\vartheta R_{dh}(\lambda,\vartheta) \quad (B.1)$$

An equivalent equation applies for light with spectrum "s".

An ideal diffuser obeys the Lambert cosine law [50], which establishes that the intensity of light diffused by the unitary surface on a unitary solid angle is: (i) proportional to the cosine of the incident angle; (ii) proportional to the cosine of the observation angle. From condition (i), considering that the illuminated area increases as $1/\cos\theta$ when the incident light is totally internal to the sample surface, it comes out that the total (d/h) reflectance, $R_{dh}(\theta,\lambda)$, is constant with the angle of incidence θ, that is:

$$R_{dh}(\theta,\lambda) = R_{dh}(8°,\lambda) = R_{dh}(\lambda) = \text{const} \quad (B.2)$$

Eq. (B.1) then becomes:

$$R_{hh}(\lambda) = 2\int_0^{\pi/2} d\vartheta \sin\vartheta\cos\vartheta R_{dh}(\lambda,8°) = \cdots 2R_{dh}(\lambda,8°)\tfrac{1}{2} = R_{dh}(\lambda,8°) \quad (B.1a)$$

An equivalent equation applies for light with spectrum "s".

By hypothesising an ideal behaviour for the Labsphere standards of reflectance, we can conclude that the $R_{dh}(\lambda,8°)$ data reported in the calibration certificate correspond to the h/h reflectance data $R_{hh}(\lambda)$.

References

[1] P. Strauss, K. Onneken, S. Krauter, Proc. 12th EC Photovoltaic Solar Energy Conference, Amsterdam, 11–15 April, 1994, H.S. Stephens & Associates, 1994, p. 1194.

[2] S. Krauter, R. Hanitsch, P. Campbell, S.R. Wenham, Proc. 12th EC Photovoltaic Solar Energy Conference, Amsterdam, 11–15 April, 1994, H.S. Stephens & Associates, 1994, p. 1198.

[3] R. Brendel, Proc. 12th EC Photovoltaic Solar Energy Conference, Amsterdam, 11–15 April, 1994, H.S. Stephens & Associates, 1994, p. 1339.

[4] A.R. Burgers, J.J. van Wijk, W.C. Sinke, Proc. 14th EC Photovoltaic Solar Energy Conference, Barcelona, 30 June–4 July, 1997, H.S. Stephens & Associates, 1997, p. 2442.

[5] J.D. Hylton, A.R. Burgers, W.C. Sinke, Proc. 14th EC Photovoltaic Solar Energy Conference, Barcelona, 30 June–4 July, 1997, H.S. Stephens & Associates, 1997, p. 139.

[6] P. Baruch, Proc. 14th EC Photovoltaic Solar Energy Conference, Barcelona, 30 June–4 July, 1997, H.S. Stephens & Associates, 1997, p. 2363.

[7] F. Zhu, P. Jennings, J. Cornish, G. Hefter, K. Luczak, Solar Energy Mater. Solar Cells 49 (1997) 163–169.

[8] P. Hanselaer, A. Van den Abeele, S. Forment, L. Frisson, J. Poortmans, Proc. 2nd World Conference on Photovoltaic Solar Energy Conversion, Wien, 6–10 July, 1998, European Commission, 1998, p. 1302.

[9] A. Boueke, R. Kuhn, M. Wibral, P. Fath, G. Wileke, E. Bucher, Proc. 2nd World Conference on Photovoltaic Solar Energy Conversion, Wien, 6–10 July, 1998, European Commission, 1998, p. 1709.

[10] N. Martin, J.M. Ruiz, Proc. 2nd World Conference on Photovoltaic Solar Energy Conversion, Wien, 6–10 July, 1998, European Commission, 1998, p. 2380.

[11] H. Nagel, A. Metz, A.G. Aberle, R. Hezel, Proc. 2nd World Conference on Photovoltaic Solar Energy Conversion,

Wien, 6–10 July, 1998, European Commission, 1998, p. 2400.
[12] R. Kuhn, A. Boneke, M. Wibral, M. Spiegel, P. Fath, G. Wieke, E. Bucher, Proc. 2nd World Conference on Photovoltaic Solar Energy Conversion, Wien, 6–10 July, 1998, European Commission, 1998, p. 2415.
[13] W. Knaupp, Proc. 22nd IEEE Photovoltaics Specialists Conference, Las Vegas, 7–11 October, 1991, IEEE, 1991, p. 620.
[14] K. Reiche, G. Kleiss, F. Lipps, R. Preu, K. Bucher, Proc. 13th EC Photovoltaic Solar Energy Conference, Nice, 23–27 October, 1995, H.S. Stephens & Associates, 1995, p. 2270.
[15] K. Bucher, Proc. 13th EC Photovoltaic Solar Energy Conference, Nice, 23–27 October, 1995, H.S. Stephens & Associates, 1997, p. 2097.
[16] K. Bucher, G. Kleiss, D. Batzner, K. Reiche. R. Preu, P. Ragot, D. Heinemann, Proc. 14th EC Photovoltaic Solar Energy Conference, Barcelona, 30 June–4 July, 1997, H.S. Stephens & Associates, 1997, p. 268.
[17] A.W. Blakers, M.J. Stocks, Proc. 14th EC Photovoltaic Solar Energy Conference, Barcelona, 30 June–4 July, 1997, H.S. Stephens & Associates, 1997, p. 305.
[18] C.W.A. Baltus, J.A. Eikelboom, R.J.C. van Zolingen, Proc. 14th EC Photovoltaic Solar Energy Conference, Barcelona, 30 June–4 July, 1997, H.S. Stephens & Associates, 1997, p. 1547.
[19] J. Wohlgemuth, J. Posbic, J. Anderson, Proc. 14th EC Photovoltaic Solar Energy Conference, Barcelona, 30 June–4 July, 1997, H.S. Stephens & Associates, 1997, p. 313.
[20] K. Bucher, Solar Energy Mater. Solar Cells 47 (1997) 85.
[21] P. Koltay, J. Wenk, K. Bucher, Proc. 2nd World Conference on Photovoltaic Solar Energy Conversion, Wien, 6–10 July, 1998, European Commission, 1998, p. 2334.
[22] N. Martin, J.M. Ruiz, Proc. 2nd World Conference on Photovoltaic Solar Energy Conversion, Wien, 6–10 July, 1998, European Commission, 1998, p. 2384.
[23] A. Parretta, A. Sarno, L. Vicari, Opt. Commun. 153 (1998) 153–163.
[24] R. Shimokawa, Y. Miyake, Y. Nakanishi, Y. Kuwano, Y. Hamakawa, Solar Cells 19 (1986–1987) 59–72.
[25] R. Preu, G. Kleiss, K. Reiche, K. Bucher, Proc. 13th EC Photovoltaic Solar Energy Conference, Nice, 23–27 October, 1995, H.S. Stephens & Associates, 1995, p. 1465.
[26] E.A. Sjerps-Koomen, E.A. Alsema, W.C. Turkenburg, Solar Energy 57 (1996) 421–432.
[27] U. Kerst, S. Krauter, R. Hanitsch, Proc. 14th EC Photovoltaic Solar Energy Conference, Barcelona, 30 June–4 July, 1997, H.S. Stephens & Associates, 1997, p. 232.
[28] N.M. Chivelet, Proc. 14th EC Photovoltaic Solar Energy Conference, Barcelona, 30 June–4 July, 1997.
[29] G. Agostinelli, E.J. Haverkamp, Proc. 2nd World Conference on Photovoltaic Solar Energy Conversion, Wien, Austria, 6–10 July, 1998. European Commission, 1998, p. 1394.
[30] B.L. Sopori, T. Marshall, IEEE, 1993, p. 127.
[31] A.R. Burgers, R. Kindermann, J.D. Hylton, W.C. Sinke, H.H.C. De Moor, Proc. 14th EC Photovoltaic Solar Energy Conference, Barcelona, 30 June–4 July, 1997, H.S. Stephens & Associates, 1997, p. 143.
[32] Y. Hishikawa, E. Maruyama, S. Yata, M. Tanaka, S. Kiyama, S. Tsuda, Solar Energy Mater. Solar Cells 49 (1997) 143–148.
[33] K. Winz, C.M. Fortmann, Th. Eickhoff, C. Beneking, H. Wagner, H. Fujinara, I. Shimizu, Solar Energy Mater. Solar Cells 49 (1997) 195–203.
[34] A.S. Al-Omar, M.Y. Ghannam, Solar Energy Mater. Solar Cells 52 (1998) 107–124.
[35] C. Zechner, G. Willeke, E. Bucher, Proc. 2nd World Conference on Photovoltaic Solar Energy Conversion, Wien, 6–10 July, 1998, European Commission, 1998, p. 1693.
[36] R.M. Hausner, R.B. Bergmann, J.H. Werner, Proc. 2nd World Conference on Photovoltaic Solar Energy Conversion, Wien, 6–10 July, 1998, European Commission, 1998, p. 1754.
[37] J.D. Hylton, A.R. Burgers, W.C. Sinke, 16th EC Photovoltaic Solar Energy Conference, Glasgow, 1–5 May, 2000.
[38] A. Parretta, A. Sarno, H. Yakubu, Opt. Commun. 161 (1999) 297–309.
[39] A. Parretta, A. Sarno, P. Tortora, H. Yakubu, P. Maddalena, J. Zhao, A. Wang, Opt. Commun. 172 (1999) 139–151.
[40] M.A. Green, Solar Cells. Operating Principles, Technology and System Application, The University of New South Wales, Kensington, Australia, 1992.
[41] M.A. Green, Silicon Solar Cells. Advanced Principles and Practice, Centre for Photovoltaic Devices and Systems, University of New South Wales, Sydney, Australia, 1995, p. 235.
[42] Patent It. A.n. RM 2000 A000634, 1 December, 2000.
[43] R. Perez, R. Seals, P. Ineichen, R. Stewart, D. Menicuzzi, Solar Energy 39 (1987) 221.
[44] R. Perez, P. Ineichen, R. Seals, J. Michalsky, R. Stewart, Solar Energy 44 (1990) 271.
[45] P. Ineichen, P. Guisan, R. Perez, Solar Energy 44 (1990) 207–214.
[46] D. Pisimanis, V. Notaridou, D.P. Lalas, Solar Energy 39 (1987) 159–172.
[47] R. Burlon, S. Bivona, C. Leone, Solar Energy 47 (1991) 83–89.
[48] N.B. Mason, T.M. Bruton, K.C. Heasman, Proc. 12th German National PV Solar Energy Symposium, OTTI Regensberg, 1997, p. 383.
[49] A.P. Brunger, F.C. Hooper, Solar Energy 51 (1993) 53–64.
[50] G. Kortum, Reflectance Spectroscopy. Principles, Methods, Applications, Springer, Berlin, 1969.
[51] A. Parretta, A. Sarno, P. Tortora, 16th EC Photobvoltaic Solar Energy Conference, 1–5 May, 2000, Glasgow, UK.
[52] A. Parretta, P. Grillo, P. Maddalena, P. Tortora, Opt. Commun. 186 (2000) 1–14.
[53] A. Maccari, M. Montecchi, F. Truppo, M. Zinzi, Appl. Opt. 37 (1998) 5156.
[54] Patent It. A.n. RM 99 A000656, 25 October, 1999.